Wnt4a Is Indispensable for Genital Duct Elongation but Not for Gonadal Sex Differentiation in the Medaka, Oryzias latipes

Authors: Kanamori, Akira, Kitani, Ryota, Oota, Atsuko, Hirano, Koudai, Myosho, Taijun, et al.

Source: Zoological Science, 40(5) : 348-359

Published By: Zoological Society of Japan

URL: https://doi.org/10.2108/zs230050

ZOOLOGICAL SCIENCE **40**: 348–359 (2023)

Wnt4a Is Indispensable for Genital Duct Elongation but Not for Gonadal Sex Differentiation in the Medaka, *Oryzias latipes*

Akira Kanamori[1]*, Ryota Kitani[1]†, Atsuko Oota[1], Koudai Hirano[1], Taijun Myosho[2], Tohru Kobayashi[2], Kouichi Kawamura[3], Naoyuki Kato[4], Satoshi Ansai[5,6,7], and Masato Kinoshita[5]

[1]*Division of Biological Science, Graduate School of Science, Nagoya University, Aichi 464-8602, Japan*
[2]*Laboratory of Molecular Reproductive Biology, Institute for Environmental Sciences, University of Shizuoka, Shizuoka 422-8526, Japan*
[3]*Department of Marine Bioresources, Graduate School of Bioresources, Mie University, Mie 514-8507, Japan*
[4]*Department of Environmental Science, Graduate School of Science and Technology, Niigata University, Niigata 950-2181, Japan*
[5]*Division of Applied Biosciences, Graduate School of Agriculture, Kyoto University, Kyoto 606-8502, Japan*
[6]*Laboratory of Bioresources, National Institute for Basic Biology, Aichi 445-8585, Japan*
[7]*Graduate School of Life Sciences, Tohoku University, Miyagi 980-8577, Japan*

In most vertebrates, the oviducts and sperm ducts are derived from the Müllerian ducts and Wolffian ducts, respectively. However, in teleosts, the genital ducts are formed by the posterior extension of gonads in both sexes. Whether the genital ducts of teleosts are newly evolved organs or variants of Müllerian ducts is an important question for understanding evolutionary mechanisms of morphogenesis. One of the genes essential for Müllerian duct formation in mice is *Wnt4*, which is expressed in the mesenchyme and induces invagination of the coelomic epithelium and its posterior elongation. Here, we addressed the above question by examining genital duct development in mutants of two Wnt4 genes in the medaka (*wnt4a* is orthologous to mouse *Wnt4*, and *wnt4b* is paralogous). The *wnt4b* mutants had a short body but were fertile with normal genital ducts. In contrast, both male and female *wnt4a* mutants had their posterior elongation of the gonads stopped within or just outside the coelom. The mutants retained the posterior parts of ovarian cavities or sperm duct primordia, which are potential target tissues of Wnt4a. The gonads of female *scl* mutants (unable to synthesize sex steroids) lacked these tissues and did not develop genital ducts. Medaka *wnt4a* was expressed in the mesenchyme ventral to the genital ducts in both sexes. Taken together, the data strongly suggest that the mouse Müllerian ducts and the medaka genital ducts share homologous developmental processes. Additionally, the *wnt4a* or *wnt4b* single mutants and the double mutants did not show sex-reversal, implying that both genes are dispensable for gonadal sex differentiation in the medaka.

Key words: Müllerian duct, evolution, sperm duct, oviduct, teleost

INTRODUCTION

In most jawed vertebrates, the oviducts and sperm ducts are derived from the Müllerian ducts (MDs) and Wolffian ducts (WDs), respectively (see Romer and Parsons, 1977; Blüm, 1986; Lombardi, 1998). However, in teleosts, both male and female genital ducts are formed by the posterior elongation of the gonads. Anatomically, there are no MDs in teleosts and the WDs (mesonephric ducts) function as nephric ducts in both sexes throughout their life cycle. Therefore, these genital ducts in teleosts have been claimed by many researchers to be completely different and non-homologous organs to the oviducts or sperm ducts of other jawed vertebrates (see above and Nagahama, 1983). We are interested in answering whether these genital ducts in teleosts are formed independently from MDs or share homologous developmental processes with MDs, which is an important question for understanding the evolutionary mechanisms of morphogenesis.

* Corresponding author. E-mail: kanamori@bio.nagoya-u.ac.jp
† Present address: Graduate School of Human Development and Environment, Kobe University, Hyogo 657-8501, Japan
doi:10.2108/zs230050

Detailed descriptions of the developmental processes of genital duct formation in teleosts are limited, except for the medaka, *Oryzias latipes* (Suzuki and Shibata, 2004). Medaka have a single gonad suspended in the coelom dorsal to the gut. In males, mature sperm are liberated in canal-like spaces within the testes, which then fuse together to from a single sperm duct primordium (referred to as a central canal). The central canal leaves the coelom, elongates further beneath the urinary bladder, and finally fuses to the urethra from its ventral side. Consequently, male medaka have a single urogenital opening (see Fig. 1; Fig. 8A for a diagram; Supplementary Movie S1). In females, the process is more intricate. Initially, the ovarian cavity forms as tissue sheets from the dorso-central somatic cells elongate laterally and join with the dorso-central elongation of the lateral periphery of the somatic tissue sheets. Ovarian lamella containing developing oocytes and oogonia are positioned ventrally to the ovarian cavity (Kanamori et al., 1985; Suzuki and Shibata, 2004). The most posterior section of the ovarian cavity lacks germ cells. The sphincter muscle beneath the urinary bladder protrudes anteriorly into the coelom from its ventral side, enveloping the lumen of the ovarian cavity to form the oviduct primordium. This primordium then elongates posteriorly within the sphincter muscle and finally opens at the dorsal base of the well-developed urogenital papillae (UGP) found in females. Further posteriorly, the urethra opens separately from the oviduct (see Fig. 3; Fig. 8D for a diagram; Supplementary Movie S2).

Cellular and molecular processes involved in MD development have been extensively documented in mice and humans, identifying approximately 20 genes as indispensable for MD formation (see Mullen and Behringer, 2014; Gonzales et al., 2021). Interestingly, the majority of these genes are expressed in both MD and WD tissues. One of the genes specifically expressed in MDs is *Wnt4*, a member of the Wnt ligand family known to function in various aspects in development (see Logan and Nusse, 2004; Steinhart and Angers, 2018; Mehta et al., 2021). *Wnt4* is expressed in the mesenchyme and induces invagination of the coelomic epithelium and posterior elongation of the MDs along the WDs (see Mullen and Behringer, 2014; Gonzales et al., 2021). Mutations of *Wnt4* lead to the absence of the MDs in mice (Vainio et al., 1999) and in humans (Biason-Lauber et al., 2004, 2007). Therefore, in this study, we generated mutants of the medaka *wnt4* homologs (*wnt4a* and *wnt4b*) and analyzed their genital duct development. The absence of any apparent phenotype may suggest an independent origin of the teleost genital ducts from MDs. Conversely, any abnormal development observed in the mutants may indicate that the development of teleost genital ducts shares some homologous developmental processes with those of MDs in jawed vertebrates.

MATERIALS AND METHODS

Medaka

Inbred strains of the medaka, HdrR, established in National Institute of Radiological Sciences, Japan (Hyodo-Taguchi and Sakaizumi, 1993), were used for *wnt4a* Δ30 mutants, and Cab, established by Carolina Biological Supply Company (Loosli et al., 2000), were used for all other mutant lines. Adults, embryos, and hatchlings were kept at 26–28°C with 14L:10D light cycle. All husbandry and experimental procedures performed in this study were approved by the Animal Care and Use Committee of Nagoya University.

wnt4a and *wnt4b* editing by CRISPR/Cas9

Target sites were selected with a web tool detecting microhomology sites (http://viewer.shigen.info/cgi-bin/crispr/crispr.cgi) (see Supplementary Figure S2). Short guide RNAs to the target sites and a Cas9 mRNA were co-injected into fertilized eggs according to Ansai and Kinoshita (2014). Homologous recombination was induced as described in Murakami et al. (2017). Details regarding the target sites, mutated alleles, and expected protein alterations can be found in Supplementary Figure S2. Injected individuals were subsequently crossed with wild type, and the resulting F_1 generation was screened to identify individuals carrying the desired mutated alleles. To ensure stable inheritance, the F_1 individuals with mutated alleles were backcrossed to wild type at least once before proceeding with incrossing of heterozygotes. The first progenies resulting from the cross between heterozygotes are referred to as G_1, and the mutants were maintained as heterozygotes. Most of the mutants can be obtained through National Bioresource Project Medaka (https://shigen.nig.ac.jp/medaka/).

Genotyping

Genomic DNA for genotyping was extracted from embryos, tail fin clips, or head tissue by alkaline lysis methods described in Ansai and Kinoshita (2014). PCR was performed with ExTaq (TaKaRa, Japan) on 2720 thermal cycler (Applied Biosystems). Amplified products were analyzed with conventional agarose gels, followed by microchip electrophoresis using the MultiNA analyzer with DNA-500 reagents (Shimadzu, Japan). This analyzer enables easy visualization of hetero-duplexed amplified DNA from both wild type and mutated alleles. In medaka, genetic sex is determined by the XX/XY system, where only the Y chromosome contains the male determining gene, dmy. To determine genetic sex, two primer pairs, 17. 19/17. 20 and 17. z1/17. z2 were used (Matsuda et al., 2002; and see Supplementary Figure S2D) to detect *dmy*. The genotyping of *wnt4a* and *wnt4b* mutant alleles was carried out as described in Supplementary Figure S2. PCR-amplified products from mutated alleles were sequenced with Big Dye terminator (v3.1) and Prism 3100 Genetic Analyzer (Applied Biosystems). The *scl* mutants were genotyped as described in Sato et al. (2008).

Morphological analyses

Histological slides were prepared by conventional methods from samples fixed with Bouin's solution, embedded in paraffin (Sigma-Aldrich, USA), serially sectioned at 7 μm, and stained with hematoxylin and eosin (Muto Pure Chemicals, Japan).

In situ hybridization

In situ hybridization was performed as described previously (Horie et al., 2016). Briefly, 7-μm paraffin sections were hydrated, treated with 1 μg/ml proteinase K (Sigma-Aldrich, USA) for 10 min at 37°C, and hybridized with DIG-labeled antisense RNA probes. Detection was done with alkaline phosphatase-labeled anti-DIG antibody and NBT/BCIP (Roche Diagnostics, USA). Control experiments with sense probes did not give detectable signals (data not shown). A near full-length cDNA of *wnt4a* (nucleotide 106–1018, GenBank# NM_001160439) was used for a probe.

RESULTS

wnt4b mutants are fertile with intact genital ducts

Wnt4 is conserved across a wide range of animal groups (see Supplementary Figure S1). Previous studies by Kossack et al. (2019) demonstrated that jawed vertebrates possess two Wnt4 genes: *wnt4a* and *wnt4b*. However, certain groups or species, such as mammals, lack the wnt4b gene. In mam-

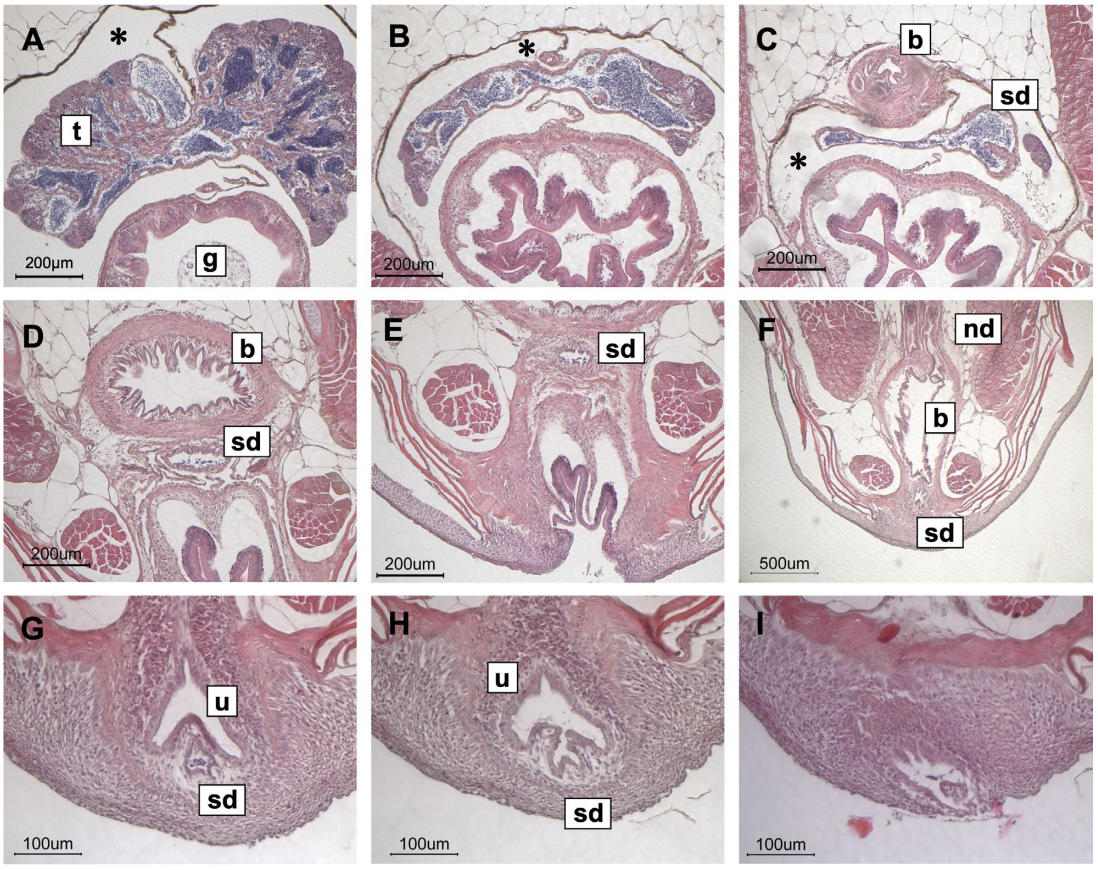

Fig. 1. Urogenital organs of a wild type male (G_6 from incrossing G_5 heterozygotes) at 4 months after hatching. Cross sections, **(A–I)**, are arranged in an anterior-to-posterior sequence. In medaka, a single testis (t) is situated centrally in the coelom (marked by asterisks) above the gut (g) **(A)**. Mature sperm were liberated from the spermatogenic cysts and were present in canal-like spaces (dark stained lumens in **[A]**), which posteriorly fused together to form larger lumens **(B)**. Further posteriorly, the lumens fused to make a single central canal (sperm duct, sd); no spermatogenic cysts were observed at this level **(C)**. Just above the coelom, anterior end of the urinary bladder (b) is shown. The sperm duct left the coelom beneath the urinary bladder **(D)**. The sperm duct is shown between the anus and the urinary bladder **(E)**. The nephric ducts (nd) are in close proximity to their eventual junction with the urinary bladder **(F)**. Subsequently, the sperm ducts fused the urethra (u) from its ventral side **(G, H)** and the urinogenital duct opened **(I)**. A sideview diagram is shown in Fig. 8A. See also Supplementary Movie S1 for the gross anatomy of the urogenital system of male medaka.

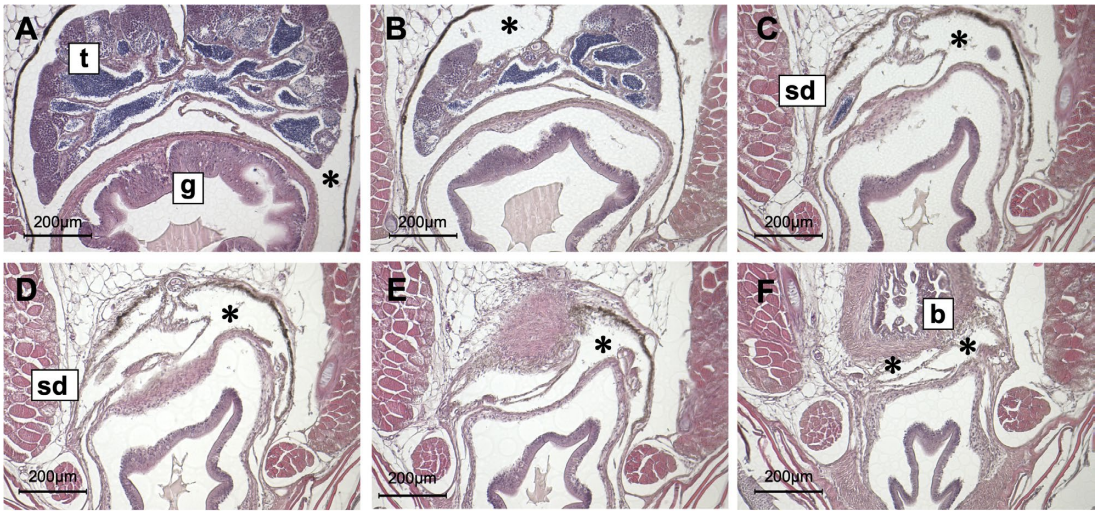

Fig. 2. Urogenital organs of a male homozygous for *wnt4a* Δ30 (G_6 from incrossing G_5 heterozygotes) at 4 months after hatching. Cross sections, **(A–F)**, are arranged in an anterior-to-posterior sequence. Spermatogenesis seemed to be progressing normally **(A)** and a sperm duct primordium (central canal) was formed posteriorly **(B, C)**. However, the primordium stopped elongating within the coelom **(D–F)**. t, testis; g, gut; sd, sperm duct (primordium); b, urinary bladder; asterisks, coelom. A sideview diagram is shown in Fig. 8B.

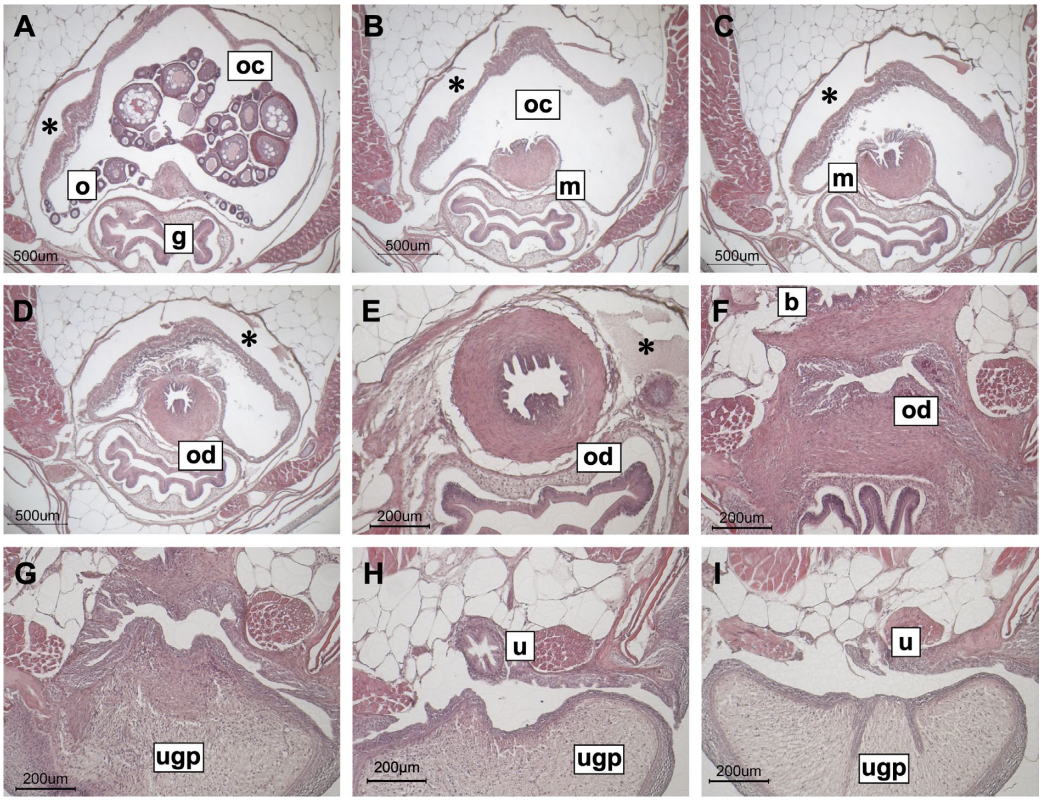

Fig. 3. Urogenital organs of a wild type female (G_6 from incrossing G_5 heterozygotes) at 4 months after hatching. Cross sections, **(A–I)**, are arranged in an anterior-to-posterior sequence. In medaka, a single ovary (o) is situated centrally in the coelom (marked by asterisks) above the gut (g) **(A)**. The ovarian lamella containing oogonia and developing oocytes were seen at the ventral side and the center of the ovarian cavity (oc). The posterior part of the ovarian cavity (oviduct primordium) did not contain germ cells and the sphincter muscle (m) protruding from posterior was seen **(B)**. A part of the ovarian cavity was enveloped by the sphincter muscle **(C)** to make the oviduct (od) posteriorly **(D, E)**. The oviduct then left the coelom, elongated under the urinary bladder (b) **(F)**, and opened dorsally at the base of the well-developed urogenital papillae (ugp) **(G)**. The urethra (u) opened separately from the oviduct between body and the ugp (I). A sideview diagram is shown in Fig. 8D. See also Supplementary Movie S2 for the gross anatomy of the urogenital system of female medaka.

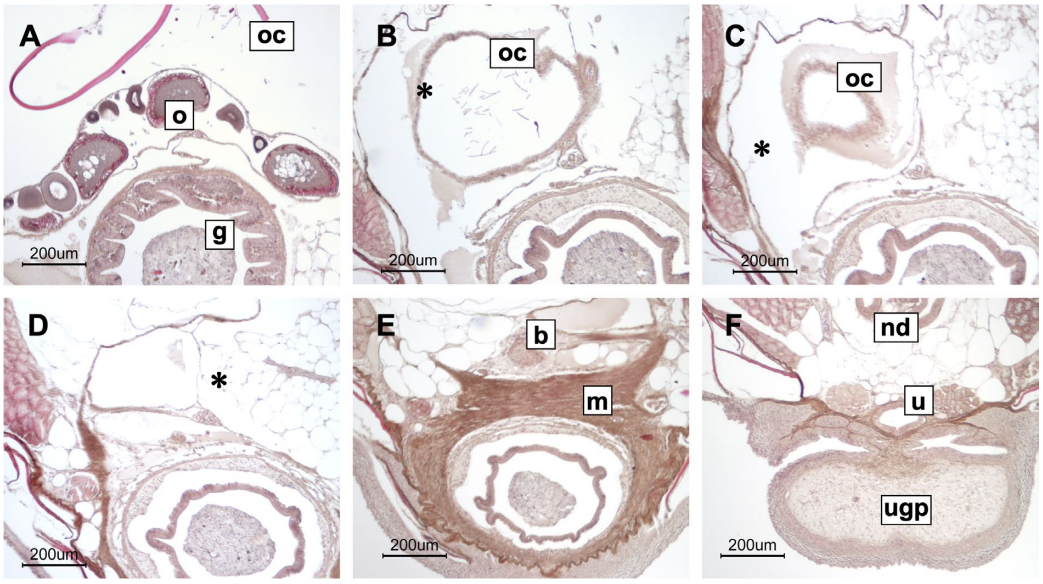

Fig. 4. Urogenital organs of a female homozygous for the *wnt4a* Δ30 (G_2 from incrossing G_1 heterozygotes) at 4 months after hatching. Cross sections **(A–F)** are arranged in an anterior-to-posterior sequence. Oogenesis seemed to be progressing normally **(A)** and a posterior portion of the ovarian cavity (oc) devoid of germ cells (oviduct primordium) was formed **(B)**. However, the primordium stopped elongating within the coelom **(C, D)**. The muscular tissue beneath the urinary bladder, well-developed urogenital papillae, and the urethra were present normally. o, ovary; g, gut; b, urinary bladder; ugp, urogenital papillae; nd, nephric duct; asterisks, coelom. A sideview diagram is shown in Fig. 8E.

mals, *Wnt4* is orthologous to medaka *wnt4a* and paralogous to medaka *wnt4b* (see Supplementary Figure S1). The phenotypes of a natural *wnt4b* mutant, characterized by reduced expression of *wnt4b* possibly due to a transposon insertion in its promoter, have been described by Inohaya et al. (2010). Similarly, our induced mutants (homozygous Δ5 and Δ29 mutants of *wnt4b*; see Supplementary Figure S2B) exhibited significantly shortened body lengths, as shown in Supplementary Figure S3. However, these mutants were fertile, and further histological examination revealed normal development of the genital ducts in both males and females (data not shown).

wnt4a Δ30 mutants lack genital ducts in both sexes

For *wnt4a* mutants, we first analyzed the *wnt4a* Δ30 allele, which has a 30 base deletion overlapping the initiation codon (see Supplementary Figure S2A). The deletion would result in the translation initiation being shifted to the second AUG codon, thereby deleting the first 11 residues of the 22-residue signal peptide. Signal peptides for secretion typically consist of N-, H-, and C-regions, all of which play crucial roles in proper secretion (see Izard and Kendall, 1994; Owji et al., 2018). The *wnt4a* Δ30 allele lacks the entire N-region containing positive-charged residues. In fact, the *wnt4a* Δ30 allele-encoded protein is not recognized as a secretion signal by a web-based prediction program (https://services.healthtech.dtu.dk/services/SignalP-6.0/). Histological analysis was conducted on adults of both sexes (3–6 months after hatching) at generations G_1, G_2, and G_6. Wild type and heterozygous males exhibited normal sperm ducts (Fig. 1; see the legends for detailed structures). In contrast, homozygous mutant males had normal testes anteriorly (Fig. 2A. B) and possessed posterior extension of the gonad devoid of germ cells (sperm duct primordia, Fig. 2C, D; asterisk in Fig. 8B) but the primordia were closed within the coelom (Fig. 2E, F). No sperm ducts were observed outside the coelom. In females also, wild type and heterozygotes had normal oviducts (Fig. 3; see the legends for detailed structures). In contrast, as in males, homozygous mutant females had normal ovaries with ovarian cavities anteriorly (Fig. 4A) and possessed posterior extension of the ovarian cavities devoid of germ cells (oviduct primordia, Fig. 4B, C; asterisk in Fig. 8E) but they were closed within the coelom (Fig. 4D). No oviducts were observed outside the coelom (Fig. 4E) and the muscular tissue was present beneath the urinary bladder. In some females, the muscular tissue was fully developed and protruded anteriorly into the coelom; the posterior lumen of the ovarian cavity was enveloped by the muscle tissue within the coelom (oviduct primordia; asterisk in Fig. 8H; and see Supplementary Figure S4). The cumulative results of both sexes are summarized in Table 1. We found one mutant male having a normal sperm duct and two heterozygous females having oviducts that were enveloped within the muscle and closed outside the coelom beneath the urinary bladder (diagrammed in Fig. 8I). These two females had only smaller oocytes, whose diameters were 200–300 μm (pre-yolk forming stages; for oocyte stages, see Iwamatsu et al., 1988), and undeveloped UGP, suggesting that they were immature females.

In addition to histological analysis, we conducted examinations of medaka urogenital organs using microCT imaging. However, it was not possible to visualize the thinnest part of the sperm ducts in males, even at the highest resolution (see Supplementary movies S1 and S2, respectively, for a male and a female). We have provided these movies and sideview diagrams (Fig. 8) to facilitate a better understanding of the anatomy of the medaka urogenital systems.

wnt4a knock-in alleles are hypomorphic

To further investigate the role of the Wnt4a gene, we generated additional mutated alleles through CRISPR/Cas9-mediated homologous recombination (see Supplementary Figure S2C). One set of the knock-in alleles contained an insertion of the mouse crystalline promoter followed by either GFP or mCherry and the SV40 polyA signal (referred to as Pcry-GFP or Pcry-mCherry). The fluorescent proteins were expressed in the lenses, making genotyping easier (see Supplementary Figure S5). Another set of knock-in alleles was created by fusing GFP or mCherry in-frame with the *wnt4a* coding sequence in the third exon (referred to as GFP-fusion or mCherry-fusion). Interestingly, the mutants with these knock-in alleles exhibited less severe phenotypes compared to the Δ30 mutants. Heterozygotes of the GFP-fusion alleles were crossed with those carrying the mCherry-fusion alleles, and the adult progenies were subjected to histological examination at G_1 and G_2. Out of eight male heterozygotes with both GFP-fusion and mCherry-fusion alleles, five exhibited closed sperm ducts outside the coelom (Fig. 5A–D; Table 2). The posterior sperm duct extended out of the coelom but remained closed beneath the urinary bladder (Fig. 5C, D). The remaining three mutants had normal sperm ducts that joined the urethra. In contrast, all female mutants, except one, with both GFP-fusion and mCherry-fusion alleles had closed oviduct primordia within the coelom, while the wild type and heterozygotes had normal oviducts. The Pcry mutants displayed the mildest phenotypes (Fig. 5E–H; Table 3). All male mutants with homozygous Pcry-GFP or Pcry-mCherry alleles, as well as two out of three Pcry-GFP/Pcry-mCherry heterozygotes, had normal sperm ducts joining the urethra. Only one of the Pcry-GFP/Pcry-mCherry heterozygotes exhibited sperm duct closure outside the coelom. In female Pcry-GFP homozygotes, Pcry-mCherry homozygotes, and Pcry-GFP/Pcry-mCherry heterozygotes, the oviduct phenotypes were approximately evenly divided among normal, closed outside the coelom, and closed within the coelom. The second phenotype was only observed in the Pcry mutants (Fig. 5G). All

Table 1. Genital duct phenotypes of the *wnt4a* Δ30 progenies (G_1, G_2, and G_6 combined).

	male			female		
	+/+	+/−	−/−	+/+	+/−	−/−
normal	9	9	1	9	7	0
closed outside the coelom	0	0	0	0	2(2)	0
closed in the coelom	0	0	8	0	0	9(1)

+/+, wild type; +/−, heterozygotes; −/−, homozygotes of *wnt4a* Δ30. Number of individuals with particular phenotypes are shown in each cell. Number within parentheses represents number of individuals with the genital duct primordium enveloped in the muscle (see Supplementary Figure S4 and Figs. 8H and 8I for diagrams).

heterozygotes exhibited normal genital ducts, regardless of the specific alleles (Table 3). In addition to the knock-in alleles, we identified deletion alleles (Δ8 and Δ14 in the third exon; see Supplementary Figure S2A) from the F_1 generation of the GFP-fusion experiments. Although the number of male mutants obtained was limited (three), both male and female mutants heterozygous for Δ8/Δ14 exhibited less severe closed genital duct phenotypes compared to the Δ30 mutants (see Supplementary Table S1).

Females of medaka *scl* mutants have intersexual gonads without genital duct primordia

As observed in the previous sections, the loss of function of *wnt4a* leads to the premature termination of posterior elongation of the genital ducts. However, the mutants still exhibited duct primordia, namely the posterior central canals in males (sperm duct primordia; asterisk in Fig. 8B) and the posterior ovarian cavities in females (oviduct primordia; asterisk in Fig. 8E). These tissues are likely to be the target tissues responsive to Wnt4a. To further address this hypothesis, the medaka *scl* mutants, which have a *17, 20-lyase* mutation and are unable to produce androgens and estrogens, were examined. Among the seven adult mutants (at 5 months after hatching) analyzed, two genetic males (XY) and one out of the five genetic females (XX sex-reversed) had normal testes with sperm ducts joining the urethra (data not shown). The remaining four XX individuals had gonads resembling ovaries, containing previtellogenic to pre-yolk forming stage oocytes (for oocyte stages, see Iwamatsu et al., 1988), along with scattered spermatogenic cysts (Fig. 6 A–D). These gonads lacked ovarian cavities, as previously described in Sato et al. (2008), as the formation of ovarian cavities depends on estrogens (Suzuki et al., 2004). Although the gonads contained some spermatogenic cysts with spermatids, no canals for sperm were found. The most posterior part of the gonads consisted only of somatic cells without lumens, and no further elongation was observed within the coelom (Fig. 6E–H; Fig. 8G for a diagram). These findings provide further support for the hypothesis that duct primordia (the posterior central canals in males and the posterior ovarian cavities in females) are the target tissues responsive to Wnt4a.

***wnt4a* is expressed below the urinary bladder during genital duct elongation**

Initially we attempted immunohistochemical detection

Table 2. Genital duct phenotypes of the *wnt4a* fusion allele progenies (G_2).

	male				female			
	+/+	+/G	+/C	G/C	+/+	+/G	+/C	G/C
normal	2	2	2	3	2	2	2	1
closed outside the coelom	0	0	0	5	0	0	0	0
closed in the coelom	0	0	0	0	0	0	0	7(2)

+/+, wild type; +/G, *wnt4a-GFP* heterozygotes; +/C, *wnt4a-mCherry* heterozygotes; G/C, *wnt4a-GFP/wnt4a-mCherry* heterozygotes. See Table 1 footnotes for explanations.

Table 3. Genital duct phenotypes of the *wnt4a* Pcry allele progenies (G_2).

	male					female				
	+/G	+/C	G/G	C/C	G/C	+/G	+/C	G/G	C/C	G/C
normal	5	2	3	4	2	2	2	1	1	2
closed outside the coelom	0	0	0	0	1	0	0	2(1)	1(1)	0
closed in the coelom	0	0	0	0	0	0	0	0	1	1

+/G, Pcry-GFP heterozygotes; +/C, Pcry-mCherry heterozygotes; G/G, Pcry-GFP homozygotes; C/C, Pcry-mCherry homozygotes; G/C, Pcry-GFP/Pcry-mCherry heterozygotes. See Table 1 footnotes for explanations.

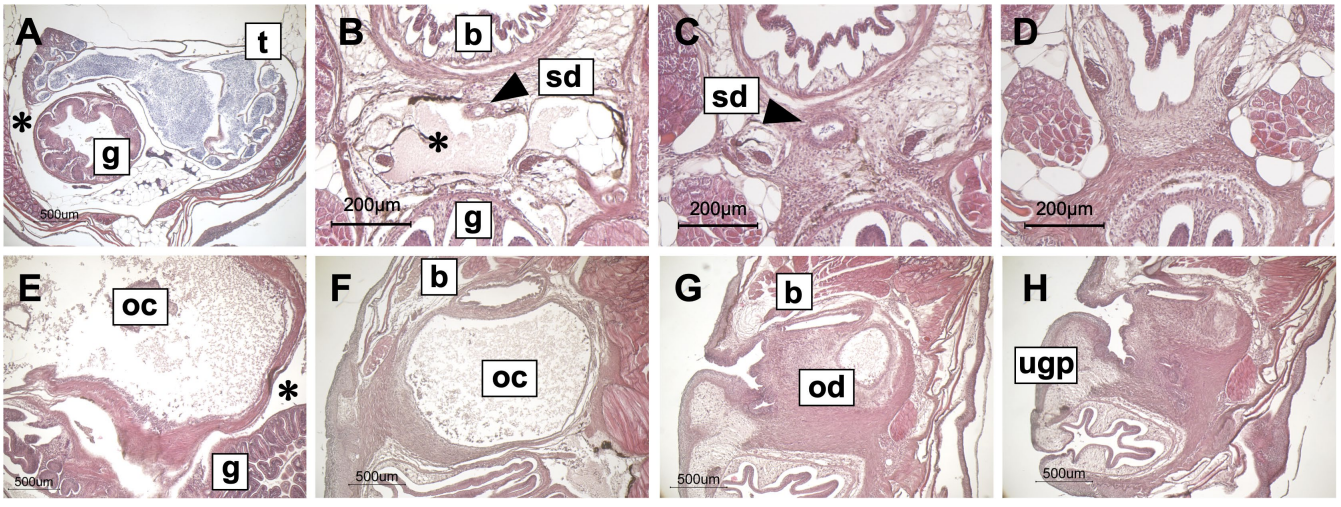

Fig. 5. Some *wnt4a* mutants of the knock-in alleles showed termination of the genital ducts outside the coelom. Cross sections, **(A–D)** for a male heterozygous for the GFP-fusion and the mCherry-fusion and **(E–H)** for a female homozygous for the Pcry-GFP, are arranged in an anterior-to-posterior sequence. The sperm duct (sd, arrowheads) or the oviduct (od) elongated outside the coelom and stopped beneath the urinary bladder (**[C, D]** for the male, **[G, H]** for the female). t, testis; g, gut; b, urinary bladder; sd, sperm duct; oc, ovarian cavity; g, gut; b, urinary bladder; ugp, urogenital papillae; asterisks, coelom. Sideview diagrams are shown in Fig. 8C and 8F for males and females, respectively.

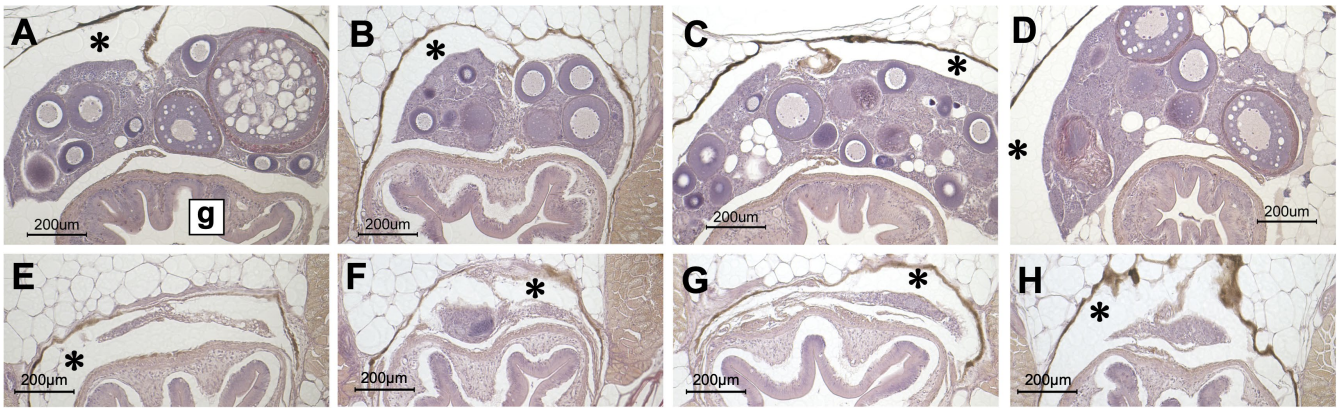

Fig. 6. Ovary-like gonads from 4 *scl* mutants of the XX adults at 5 months after hatching. Cross sections of the posterior part of the gonads containing previtellogenic to pre-yolk forming stage oocytes with scattered spermatogenic cysts; no ovarian cavities or canals for sperm were formed **(A–D)**. The posterior end of the gonads contained only somatic cells without lumens **(E–H)**. **(A–D)** and **(E–H)** are from the same individuals, respectively. g, gut; asterisks, coelom. A sideview diagram is shown in Fig. 8G.

with GFP antibodies on medaka with the *wnt4a* GFP-fusion allele. However, we could not obtain reliable signals. Next, we used conventional in situ hybridization and detected signals on mesenchyme beneath the sperm ducts and epithelium of the sperm duct in males (Fig. 7A) and mesenchyme beneath oviducts and the periphery of the sphincter muscle in females (Fig. 7B). The control sense probes did not give any detectable signals (Fig. 7C, D). In the gonads, spermatids and spermatozoa were stained because of their intrinsic alkaline phosphatase activities (Fig. 7E) and the developing oocytes exhibited positive signals (Fig. 7F); We did not detect positive signals on the gonadal somatic cells in either sex (Fig. 7E, F).

No sex-reversals in *wnt4* mutant medaka

The role of WNT4 in ovarian differentiation is well established in mammals (Vainio et al., 1999; see also Bernard and Harley, 2007; Nicol and Yao, 2014); *Wnt4* mutant females show partial sex-reversals. In teleosts, zebrafish *wnt4a* mutants showed a higher male ratio than the wild type (Kossack et al., 2019). Therefore, we examined whether sex-reversal occurs in *wnt4* medaka mutants. First, we checked eight genetic males (XY) and eight genetic females (XX) homozygous for the *wnt4b* Δ29 allele and found no sex-reversals. Genetic sex was confirmed by the presence or absence of *dmy*, the male-determining gene of medaka with two independent primer pairs (see Supplementary Figure S2D). Phenotypic sex was determined based on the external morphology of the dorsal and anal fins and the UGP, together with the gross morphology of the gonads. For *wnt4a*, the Δ30 allele and the fusion alleles were examined and no significant sex-reversals were identified (see Supplementary Table S2). Since the *wnt4b* mutants are fertile, the G_6 females homozygous for the *wnt4b* Δ29 or Δ5 alleles were crossed with the G_6 males heterozygous for the *wnt4a* Δ30 allele. Progenies heterozygous for both *wnt4a* and *wnt4b* were incrossed to generate *wnt4a* and *wnt4b* double mutants. As the *wnt4b* mutant phenotype (shorter body) can be detectable at 1 week after hatching, we only selected *wnt4b* homozygotes for further analyses. In adults (3–6 months after hatching), we examined the genotypes (*dmy*, *wnt4a*, and *wnt4b*) and phenotypes (fins, UGP, and gonads)

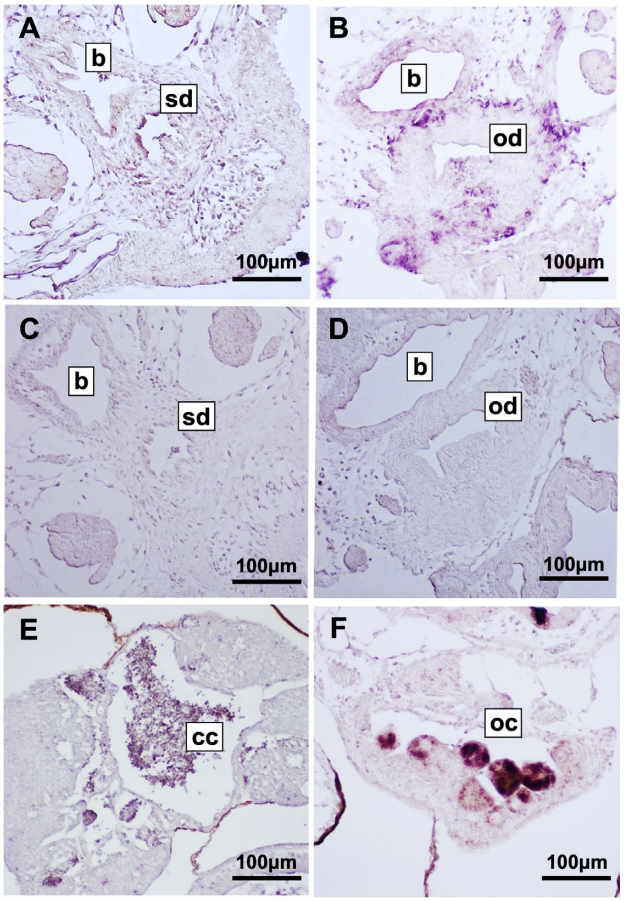

Fig. 7. In situ hybridization of *wnt4a*. The cross sections of a male and a female at 70 days after hatching were hybridized to an antisense RNA probe. Signals were detected on the mesenchyme beneath the sperm ducts and the epithelium of the sperm duct in the male **(A)** and the mesenchyme beneath the oviducts and the periphery of the sphincter muscle in the female **(B)**. The control sense probes did not give any detectable signals **(C, D)**. In the gonads, spermatids and spermatozoa were stained because of their intrinsic alkaline phosphatase activities **(E)** and the developing oocytes exhibited positive signals **(F)**. We did not detect positive signals on the gonadal somatic cells in either sex. b, urinary bladder; sd, sperm duct; od, oviduct; cc, central canal; oc, ovarian cavity.

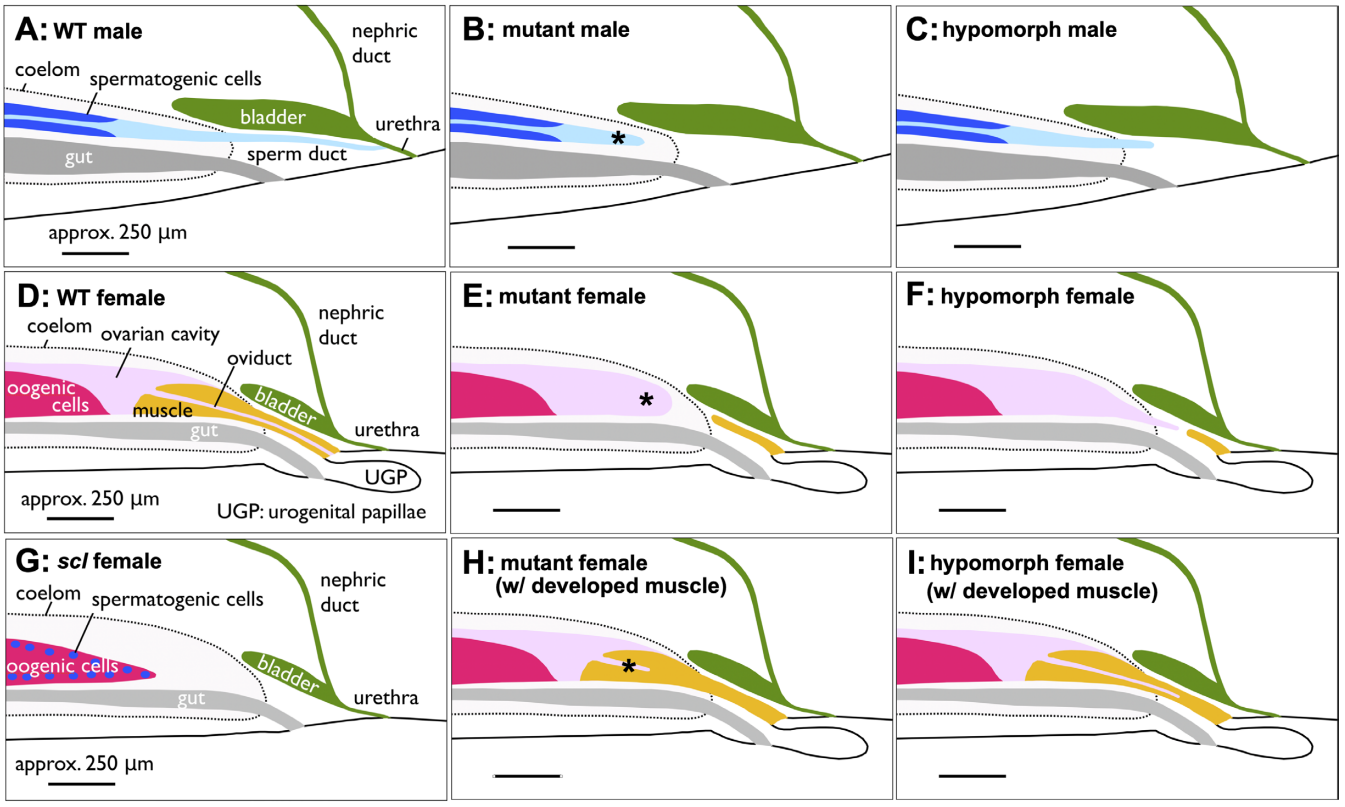

Fig. 8. Median plane (sideview) diagrams illustrating urogenital organs in wild type and *wnt4a* mutant medaka. The diagrams were roughly reconstructed from the serial histological sections. **(A, D)** wild type male and female, respectively. **(B, E)** mutant male and female with sperm duct closed in the coelom, respectively. **(C, F)** mutant male and female with sperm duct closed outside the coelom, respectively. **(G)** XX *scl* mutant with ovary-like gonad. **(H, I)** female mutants with developed sphincter muscle protruded into the coelom. The oviducts are closed within and outside the coelom, respectively. The genital duct primordia are marked with asterisks in the mutants **(B, E, H)**.

Table 4. Number of sex-reversals in the *wnt4a* and *wnt4b* double mutants.

	wnt4b Δ29/Δ29			*wnt4b* Δ5/Δ5		
wnt4a Δ30	+/+	+/−	−/−	+/+	+/−	−/−
XY female	0/3	0/16	0/18	0/7	0/15	0/6
XX male	0/3	0/17	0/12	0/12	1/29	0/11

+/+, wild type; +/−, heterozygotes; −/−, homozygotes of *wnt4a* Δ30. Number of sex-reversals with particular phenotypes/total number of samples examined are shown in each cell.

as described above. The results presented in Table 4 indicate no significant occurrence of sex-reversals in the double mutants. Genital duct phenotypes were further examined histologically for some of these individuals. There seemed to be no additional effect of the *wnt4b* mutation, either Δ29 or Δ5, on the *wnt4a* Δ30 mutation (see Supplementary Table S3). We did not identify significant differences; most of the *wnt4a* and *wnt4b* double mutants had their genital ducts closed in the coelom similar to the *wnt4a* Δ30 single mutants (Table 1).

DISCUSSION

wnt4a but not *wnt4b* is indispensable for genital duct elongation in male and female medaka

The *wnt4a* Δ30 homozygous mutants of both sexes showed premature termination of genital duct elongation in the coelom (Figs. 1–4; Table1). The mutants carrying *wnt4a* knock-in alleles also displayed similar, albeit less severe, phenotypes (Fig. 5; Tables 2–4, and see Supplementary Table S1). Together, these results strongly indicate that in medaka, *wnt4a* is indispensable for genital duct elongation in both sexes. The *wnt4b* medaka mutants had normal genital ducts in both sexes. Similar anomalies of genital duct formation in *wnt4a* mutants were reported in another teleost, zebrafish (Kossack et al., 2019). The male mutants had sperm duct primordia but the left and right primordia did not fuse and elongate posteriorly. The female mutants also had undeveloped oviduct primordium, which did not elongate posteriorly. Expression of *wnt4a* was detected in the mesenchyme beneath the nephric ducts in both sexes in zebrafish (Kossack et al., 2019). Here, in medaka, we also detected *wnt4a* expression in the mesenchyme beneath the urinary bladder in both sexes. Taken together, these findings that *wnt4a* is expressed in the mesenchyme in both medaka and zebrafish (two relatively diverged teleost species) suggest a hypothesis that Wnt4 directly or indirectly acts on the duct primordia to induce their posterior elongation. If this hypothesis is correct, the lack of the genital duct primordia should lead to the absence of the genital ducts. The female *scl* mutants did not develop the duct primordia (the posterior central canals and the posterior ovarian cavities) and completely lacked genital ducts (Figs. 6; 8G). The results further

support the above hypothesis.

It should be noted that Wnt signals typically propagate over short distances, spanning only a few cell lengths (see Logan and Nusse, 2004; Steinhart and Angers, 2018; Mehta et al., 2021). Here, the possible target tissue is located within the coelom. Therefore, how Wnt4a signals, directly or indirectly, act via coelomic fluid is unknown. Wnt proteins, either in canonical or non-canonical pathways, exert their influence via frizzled receptors on the cell membrane followed by recruitment of cytoplasmic dishevelled proteins. We have not examined expression of these proteins in the medaka genital duct primordia. The involvement of these proteins in mammalian MD development has only been sparsely documented (see Mullen and Behringer, 2014; Gonzales et al., 2021).

Hypomorphic phenotypes may be caused by transcriptional adaptation

Unexpected results were obtained from the knock-in mutants by the Pcry-alleles and the fusion-alleles, where DNA constructs were inserted in the third exon. Despite the anticipated loss of protein function from these alleles (see Supplementary Figure S2C), their mutants showed milder phenotypes compared to the Δ30 homozygous mutants (Tables 1–3). Notably, most of the male mutants by the Pcry-alleles displayed normal sperm duct development. These findings could be attributed to a phenomenon known as transcriptional adaptation (El-Brolosy et al., 2019; see also Jakutis and Stainier, 2021). Premature termination codons in mutated genes often trigger mRNA degradation via nonsense-mediated mRNA decay (see Lykke-Andersen and Jensen, 2015; Nagar et al., 2023). Consequently, small RNA fragments derived from the degraded mRNA induce transcriptional upregulation of genes with similar sequences, referred to as adapting genes. In the *wnt4a* knock-in mutants, potential candidates for adapting genes include *wnt4b* or other Wnt genes. Both the Pcry-alleles and the fusion-alleles harbor premature termination codons in the third exon, which may activate nonsense-mediated mRNA decay (see Supplementary Figure S2C).

The function of Wnt4a may be sex and stage dependent

The phenotypes of the Δ30 homozygous mutants were largely consistent between the two sexes (Table 1). However, this was not the case for other knock-in mutants. In the Pcry mutants, the males exhibited normal genital ducts, whereas approximately half of the females displayed impaired elongation of the oviducts (Table 3). Similarly, in the homozygous mutants of the fusion alleles, most females exhibited closed genital duct phenotypes, while approximately half of the males showed normal sperm ducts (Table 2). These results suggest that females may require higher Wnt4a activity for genital duct formation compared to males. Alternatively, the activity of Wnt4a in the knock-in mutants may be higher in males than in females. Furthermore, our observations revealed that closure of the genital ducts occurred outside the coelom in the knock-in mutants, with the posterior ends of the ducts ceasing their elongation beneath the urinary bladder (Tables 2 and 3). These phenotypes were observed in both sexes and suggest that Wnt4a signals are necessary for at least two steps in the process of genital duct elongation: initial elongation of the duct primordia within the coelom and subsequent posterior elongation beneath the urinary bladder. Further investigations at the cellular and molecular levels are required to elucidate the mechanisms underlying the processes of genital duct elongation.

Possible homology between developmental processes of teleost genital ducts and MDs

In mice, *Wnt4* KO completely abrogates invagination of the coelomic epithelium and posterior elongation of the MDs (Vainio et al., 1999). In teleosts, zebrafish (Kossack et al., 2019) and medaka (the present study), posterior elongation of the genital duct primordia was inhibited by *wnt4a* (ortholog of mammalian *Wnt4*) KO in both sexes. In female teleosts, the epithelium lining the oviducts is continuous with the epithelium facing the ovarian cavities, which is derived from the coelomic epithelium (see Nagahama, 1983; Kanamori et al., 1985). In contrast, the epithelium facing the sperm duct lumen is continuous with the epithelium lining the central canals, which is derived from the Sertoli cells (see Nagahama, 1983; Kanamori et al., 1985). The origin of the Sertoli cells in medaka is the lateral plate mesoderm (Nakamura et al., 2006), but there is no conclusive research showing their origin to be the coelomic epithelium. Kanamori et al. (1985) described a group of somatic cells with a distinct basal lamina in the developing medaka gonads; they develop into the Sertoli cells and the epithelial cells lining the sperm duct in males and the epithelial cells lining the ovarian cavities in addition to the granulosa cells in females. In mice, the Sertoli cells have been shown to originate from the coelomic epithelium (Karl and Capel, 1999).

The similarities observed in Wnt4 (Wnt4a) mutants between mammals and teleosts strongly suggest the existence of homologous processes in genital duct formation in both groups. However, significant differences exist in the duct shapes and their relationships to the coelom. In mice, the anterior coelomic epithelium is invaginated, whereas in teleosts, the genital duct primordia within the gonads elongate posteriorly and exit the coelom at the most posterior end (Fig. 9 for diagrams). These teleost-specific derived characteristics make interpreting the homology challenging. Alternatively, it is possible that teleost *wnt4a* and mammalian *Wnt4* have been co-opted during evolution for MD and genital duct formation, respectively. To further investigate the potential homology, we propose two approaches. The first approach involves detailed molecular and cellular studies of medaka genital duct elongation. We may be able to find common genetic networks between medaka and mice, where detailed studies have already been reported (see Mullen and Behringer, 2014; Gonzales et al., 2021). During preliminary in situ hybridization experiments in the genital duct primordia, we examined expression of the medaka orthologs of *Pax2*, *Lhx1*, and *Emx2*, all of which are expressed in the mammalian MD epithelium, and did not get positive signals. The second approach takes an evolutionary developmental biology (evo-devo) perspective. Studies on sturgeon (Wrobel, 2003), caecillian (limbless amphibian, Wrobel and Süß, 2000), birds (Guioli et al., 2007), and mammals (Guioli et al., 2007; see also Mullen and Behringer, 2014 and Gonzalez et al., 2021) have indicated that their

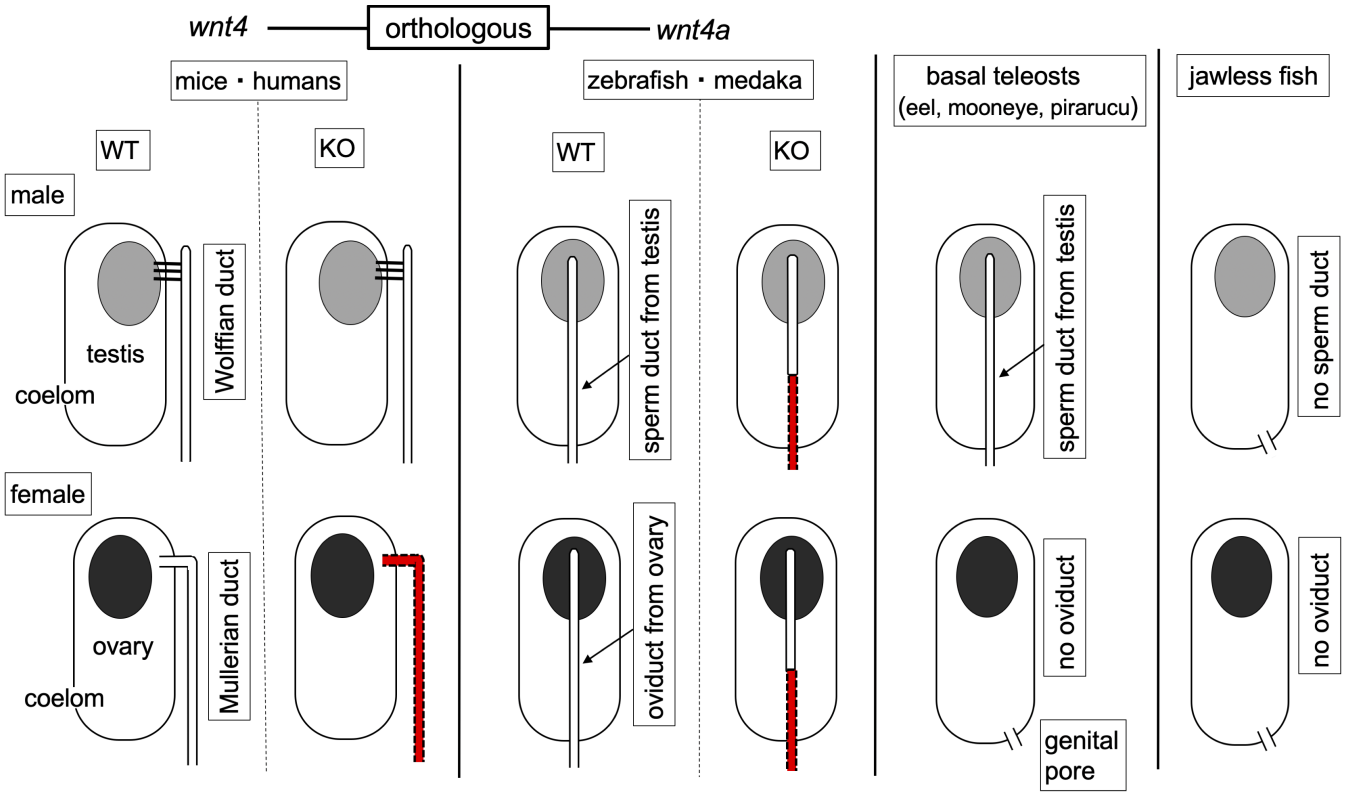

Fig. 9. Diagrams of genital ducts (pores) in various vertebrates and effects of Wnt4 (Wnt4a) mutations (KO). Frontal views with anterior side up. The mutants in orthologous genes, *Wnt4* in mammals (mice and humans) and *wnt4a* in teleosts (zebrafish and medaka), show defective development in the MD and the genital ducts, respectively (missing tissue shown in red), suggesting the presence of homologous developmental processes. In jawless fish of both sexes and females of the basal teleosts, genital ducts are absent, and the gametes are released through the genital pores instead.

MDs develop through invagination of the coelomic epithelium followed by posterior elongation. Cartilaginous fishes, including sharks and rays, were the first to evolve MDs. However, in these species, the pronephric ducts themselves differentiate into MDs, and WDs (nephric ducts) develop through longitudinal splitting of the pronephric ducts (see Wourms, 1977; Romer and Parsons, 1977; Goodrich, 1930). This remarkable difference requires further explanation at the cellular and molecular levels to understand the underlying mechanisms. On the other hand, jawless fish such as hagfish and lamprey do not possess genital ducts. Instead, mature sperm or eggs are released into the coelom and exit through the genital pores. These pores are induced by sex steroids and formed through apparent apoptosis of 2–3 layers of cells between the coelom and the urogenital sinus (Knowles, 1939). The homology of these genital pores to MDs has been a subject of debate (see Goodrich, 1930). Additionally, in basal teleosts such as eels (Tesch, 1977; Fishelson, 1992), mooneye (Katechis et al., 2007), and pirarucu (Godinho et al., 2005), the females lack genital ducts but possess genital pores similar to those found in jawless fish. However, the males in these species do have sperm ducts.

Currently, there is limited information available on the cellular and molecular processes involved in the development of genital ducts (pores) in vertebrates, except for mammals. Conducting comprehensive studies on their development in diverse vertebrate groups, coupled with exploring the potential role of Wnt4 (Wnt4a), can provide further evidence of homology and valuable insights into the evolutionary aspects of genital ducts (pores) across vertebrates.

Gonadal sex differentiation of medaka is not dependent on Wnt4a

The loss of WNT4 activities causes partial female-to-male sex-reversal in mammals (Vainio et al., 1999; see also Bernard and Harley, 2007; Nicol and Yao, 2014). Previous studies revealed that WNT4 proteins act on gonadal supporting cells to repress the transcription of *sox9*, thereby switching these cells toward the female pathway. In teleosts, knock out of *wnt4a* (the ortholog of mammalian *Wnt4*) in zebrafish caused a higher male ratio than that in the wild type (Kossack et al., 2019). Those authors demonstrated that, besides being expressed in the mesenchyme beneath the nephric ducts, *wnt4a* is also expressed in the ovarian somatic cells during gonadal sex differentiation in zebrafish. In contrast, we did not observe any effect of *wnt4a* knockout on gonadal sex differentiation in medaka. The double knockout of *wnt4a* and *wnt4b* also did not affect gonadal sex differentiation in medaka. In our study, we did not detect *wnt4a* signals in the gonadal somatic cells of medaka. The difference in the function of Wnt4a in gonadal sex differentiation between medaka and zebrafish may be due to the genetic sex determination of medaka (Aida, 1921; Matsuda et al., 2002), which is different from the environmental sex determination observed in zebrafish (see Kossack and Draper,

2019).

In conclusion, we found that medaka *wnt4a* mutants have their genital ducts stopped within the coelom or just after leaving the coelom in both sexes. These findings, combined with similar phenotypes observed in zebrafish, support the existence of homologous developmental processes between mammalian MDs and teleost genital ducts.

ACKNOWLEDGMENTS

The authors thank the following for their help: Mr. K. Kubo for histology and genotyping; Dr. H. Hori for genotyping by MultiNA; Dr. H. Hashimoto for medaka *wnt4a* cDNA plasmids; Dr. R. Araki for microCT analyses; National Bioresource Project Medaka (https://shigen.nig.ac.jp/medaka/), especially Dr. M. Matsuda for supplying *scl* mutants. This work was supported in part by a Grant-in-Aid for Scientific Research from JSPS (19K06738 to AK).

COMPETING INTERESTS

The authors declare that there are no conflicts of interest.

AUTHOR CONTRIBUTIONS

SA, MK, and AO designed and performed CRISPR knockout. TM and TK performed in situ hybridization. KK analyzed phylogeny of Wnt4. NK performed skeletal staining. RK, AO, KH, and AK performed all of the other experiments. AK conceived the study and wrote the manuscript.

SUPPLEMENTARY MATERIALS

Supplementary materials for this article are available online. (URL: https://doi.org/10.2108/zs230050)

Supplementary Figure S1. Phylogeny of animal Wnt4 proteins.

Supplementary Figure S2. The mutated alleles of *wnt4a* and *wnt4b* obtained by CRISPR/Cas9.

Supplementary Figure S3. Wild type (+/+) and *wnt4b* Δ29 mutant (−/−) medaka (G_2 from incrossing G_1 heterozygotes) stained with Alizarin Red S.

Supplementary Figure S4. Urogenital organs of a female homozygous for the *wnt4a*Δ30 (G_2 from incrossing G_1 heterozygotes) at 4 months after hatching.

Supplementary Figure S5. Embryos from crosses between the Pcry-GFP heterozygotes and the Pcry-mCherry heterozygotes at 6 days after fertilization.

Supplementary Table S1. Genital duct phenotypes of the *wnt4a* Δ8 and Δ14 progenies (G_1 and G_2 combined).

Supplementary Table S2. Number of sex-reversals in the *wnt4a* mutants (Δ30 and fusion alleles).

Supplementary Table S3. Genital duct phenotypes of the *wnt4a* and *wnt4b* double mutants.

Supplementary Movie S1. Gross anatomy of the urogenital system of male medaka.

Supplementary Movie S2. Gross anatomy of the urogenital system of female medaka.

REFERENCES

Aida T (1921) On the inheritance of color in a fresh-water fish, *Aplocheilus latipes* Temmick and Schlegel, with special reference to sex-linked inheritance. Genetics 6: 554–573

Ansai S, Kinoshita M (2014) Targeted mutagenesis using CRISPR/Cas system in medaka. Biol Open 3: 362–371

Bernard P, Harley VR (2007) Wnt4 action in gonadal development and sex determination. Int J Biochem Cell Biol 39: 31–43

Biason-Lauber A, Konrad D, Navratil F, Schoenle EJ (2004) A WNT4 mutation associated with Müllerian-duct regression and virilization in a 46, XX woman. N Engl J Med 351: 792–798

Biason-Lauber A, De Filippo G, Konrad D, Scarano G, Nazzaro A, Schoenle EJ (2007) WNT4 deficiency – a clinical phenotype distinct from the classic Mayer-Rokitansky-Kuster-Hauser syndrome: a case report. Hum Reprod 22: 224–229

Blüm V (1986) Vertebrate Reproduction. Springer Verlag, Berlin

El-Brolosy MA, Kontarakis Z, Rossi A, Kuenne C, Günther S, Fukuda N, et al. (2019) Genetic compensation triggered by mutant mRNA degradation. Nature 568: 193–197

Fishelson L (1992) Comparative gonad morphology and sexuality of the Muraenidae (Pisces, Teleostei). Copeia 1992: 197–209

Godinho HP, Santos JE, Formagio PS, Guimarães-Cruz RJ (2005) Gonadal morphology and reproductive traits of the Amazonian fish *Arapaima gigas* (Schinz, 1822). Acta Zool 86: 289–294

Gonzalez LS, Rota IA, Artibani M, Morotti M, Hu Z, Wietek N, et al. (2021) Mechanistic drivers of Müllerian duct development and differentiation into the oviduct. Front Cell Dev Biol 9: 605301

Goodrich ES (1930) Studies on the structure and development of vertebrates. Macmillan, London

Guioli S, Sekido R, Lovell-Badge R (2007) The origin of the Mullerian duct in chick and mouse. Dev Biol 302: 389–398

Horie Y, Myosho T, Sato T, Sakaizumi M, Hamaguchi S, Kobayashi T (2016) Androgen induces gonadal soma-derived factor, Gsdf, in XX gonads correlated to sex-reversal but not Dmrt1 directly, in the teleost fish, northern medaka (*Oryzias sakaizumii*). Mol Cell Endocrinol 436: 141–149

Hyodo-Taguchi Y, Sakaizumi M (1993) List of inbred strains of the medaka, *Oryzias latipes*, maintained in the Division of Biology, National Institute of Radiological Sciences. The Fish Biology Journal MEDAKA 5: 29–30

Inohaya K, Takano Y, Kudo A (2010) Production of Wnt4b by floor plate cells is essential for the segmental patterning of the vertebral column in medaka. Development 137: 1807–1813

Iwamatsu T, Ohta T, Oshima E, Sakai N (1988) Oogenesis in the medaka *Oryzias latipes* – stages of oocyte development. Zool Sci 5: 353–373

Izard JW, Kendall DA (1994) Signal peptides: exquisitely designed transport promoters. Mol Microbiol 13: 765–773

Jakutis G, Stainier DYR (2021) Genotype-Phenotype Relationships in the Context of Transcriptional Adaptation and Genetic Robustness. Annu Rev Genet 55: 71–91

Kanamori A, Nagahama Y, Egami N (1985) Development of the tissue architecture in the gonads of the medaka *Oryzias latipes*. Zool Sci 2: 695–706

Karl J, Capel B (1998) Sertoli cells of the mouse testis originate from the coelomic epithelium. Dev Biol 203: 23–33

Katechis CT, Sakaris PC, Irwin ER (2007) Population demographics of *Hiodon tergisus* (Mooneye) in the Lower Tallapoosa River. Southeast Nat 6: 461–470

Knowles FGW (1939) The influence of anterior-pituitary and testicular hormones on the sexual maturation of lampreys. J Exp Biol 16: 535–547

Kossack ME, Draper BW (2019) Genetic regulation of sex determination and maintenance in zebrafish (*Danio rerio*). Curr Top Dev Biol 134: 119–149

Kossack ME, High SK, Hopton RE, Yan Y, Postlethwait JH, Draper BW (2019) Female sex development and reproductive duct formation depend on Wnt4a in zebrafish. Genetics 211: 219–233

Logan CY, Nusse R (2004) The Wnt signaling pathway in development and disease. Annu Rev Cell Dev Biol 20: 781–810

Lombardi J (1998) Comparative Vertebrate Reproduction. Kluwer Academic Publishers, Boston

Loosli F, Köster RW, Carl M, Kühnlein R, Henrich T, Mücke M, et al. (2000) A genetic screen for mutations affecting embryonic development in medaka fish (*Oryzias latipes*). Mech Dev 97: 133–139

Lykke-Andersen S, Jensen TH (2015) Nonsense-mediated mRNA decay: An intricate machinery that shapes transcriptomes. Nat

Rev Mol Cell Biol 16: 665–677
Matsuda M, Nagahama Y, Shinomiya A, Sato T, Matsuda C, Kobayashi T, et al. (2002) DMY is a Y-specific DM-domain gene required for male development in the medaka fish. Nature 417: 559–563
Mehta S, Hingole S, Chaudhary V (2021) The Emerging Mechanisms of Wnt Secretion and Signaling in Development. Front Cell Dev Biol 16: 714746
Mullen RD, Behringer RR (2014) Molecular genetics of Müllerian duct formation, regression and differentiation. Sex Dev 8: 281–296
Murakami Y, Ansai S, Yonemura A, Kinoshita M (2017) An efficient system for homology-dependent targeted gene integration in medaka (*Oryzias latipes*). Zool Lett 3: 10
Nagahama Y (1983) The functional morphology of teleost gonads. In "Fish Physiology vol. 9 pt. A" Ed by WS Hoar, DJ Randall, EM Donaldson, Academic Press, New York, pp 223–264
Nagar P, Islam MR, Rahman MA (2023) Nonsense-mediated mRNA decay as a mediator of tumorigenesis. Genes (Basel) 14: 357
Nakamura S, Kobayashi D, Aoki Y, Yokoi H, Ebe Y, Wittbrodt J, et al. (2006) Identification and lineage tracing of two populations of somatic gonadal precursors in medaka embryos. Dev Biol 295: 678–688
Nicol B, Yao HH (2014) Building an ovary: insights into establishment of somatic cell lineages in the mouse. Sex Dev 8: 243–251
Owji H, Nezafata N, Negahdaripoura M, Hajiebrahimia A, Ghasemia Y (2018) A comprehensive review of signal peptides: Structure, roles, and applications. Eur J Cell Biol 97: 422–441
Romer AS, Parsons TS (1977) The Vertebrate Body. 5th ed, W. B. Saunders Co., Philadelphia
Sato T, Suzuki A, Shibata N, Sakaizumi M, Hamaguchi S (2008) The novel mutant *scl* of the medaka fish, *Oryzias latipes*, shows no secondary sex characters. Zool Sci 25: 299–306
Steinhart Z, Angers S (2018) Wnt signaling in development and tissue homeostasis. Development 145: dev146589
Suzuki A, Shibata N (2004) Developmental process of genital ducts in the medaka, *Oryzias latipes*. Zool Sci 21: 397–406
Suzuki A, Tanaka M, Shibata N (2004) Expression of *Aromatase* mRNA and effects of aromatase inhibitor during ovarian development in the medaka, *Oryzias latipes*. J EXp Zool A Comp Exp Biol 301: 266–273
Tesch FW (1977) The Eel. Chapman and Hall Ltd., New York
Vainio S, Heikkilä M, Kispert A, Chin N, McMahon AP (1999) Female development in mammals is regulated by Wnt-4 signalling. Nature 397: 405–409
Wourms JP (1977) Reproduction and development in Chondrichthyan fishes. Amer Zool 17: 379–410
Wrobel KH (2003) The genus *Acipenser* as a model for vertebrate urogenital development: the Müllerian duct. Anat Embryol 206: 255–271
Wrobel KH, Süß F (2000) The significance of rudimentary nephrostomial tubules for the origin of the vertebrate gonad. Anat Embryol 201: 273–290

(Received June 12, 2023 / Accepted July 24, 2023 /
Published online September 29, 2023)